Research Article

Advances in Theoretical & Computational Physics

# Impact of π-π Interaction Mode and Vinylene Bond Geometry on Helical Wrapping of Carbon Nanotubes

**Rosi N Gunasinghe[1]*, Ryza N Musin[2], Duminda K Samarakoon[2], Yi Pang[3] and Xiao-Qian Wang[2]***

[1]*Department of Chemistry and Biochemistry*

[2]*Department of Physics*

[3]*Department of Chemistry*

***Corresponding author**

Rosi N Gunasinghe, Department of Chemistry and Biochemistry, University of North Georgia, Gainesville, GA 30566 USA; E-mail: rosi.gunasingh@ung.edu

Xiao-Qian Wang, Department of Physics, Clark Atlanta University, Atlanta, GA 3014, USA; E-mail: xwang@cau.edu

**Submitted**: 18 Apr 2018; **Accepted**: 25 Apr 2018; **Published**: 30 May 2018

## Abstract

*Recent experimental work demonstrates that the parallel displaced (P) and the Y-shaped conformations of the benzene dimer are favorable over the previously assumed lowest energy configuration. Here we report on a systematical study on various conformations of the benzene dimer in excellent agreement with experimental observations. The study also demonstrates the important role of dispersion forces on the structural and electronic stability of parallel displaced and Y-shaped conformations. Our results provide important insight into the nature of π-π interactions. The corresponding conformational effects of π-conjugated polymers on the helical wrapping of single-walled carbon nanotubes are studied using dispersion-corrected density-functional calculations. The effective dispersion of nanotubes depends on the helical pitch length associated with the conformations of linkages as well as π-π stacking configurations. Our electronic structure calculation results reveal that long-range dispersive forces play a significant role in determining the relative stability of T-shaped, Y-shaped, and parallel-displaced P configurations. The implications of dispersion mechanism and future nanotube separations are discussed.*

**Keywords:** Conformations, Helical Wrapping, Density-Functional Theory, π-π interaction, Long-range dispersive forces, Carbon nanotubes.

## Introduction

Carbon nanotubes (CNTs) represent an intriguing class of materials currently being utilized for the exploration of nanostructured composites as well as applications in nanoerlectronics [1-3]. Undoped single-walled carbon nanotubes (SWCNTs) ae unique among solid-state materials because of their unmatched characteristics arising from both metallic and semiconductingSWCNTs [4]. However, as-synthesized samples inevitably yield mixed bundles of metallic and semiconducting tubes [5,6]. It is necessary to develop proper dispersion methods to obtain pure SWCNTs for fabrication of nanoelectronic devices. The solubilization of SWCNTs can be achieved via covalent sidewall functionalization, which involves the destruction of C-C bonds on tubes and may lead to deterioration of both mechanical and electronic properties [5]. On the other hand, non-covalent supramolecular modifications involve polymer wrapping on the surfaces of SWCNTs, preserving desired properties [5]. Chiral-selective reactivity and redox chemistry of CNTs are promising methods for the development of techniques that isolate CNTs into pure samples of a single electronic type and promote reversible doping of CNTs for electronic applications [7-12]. Since π-conjugated polymer wrapping around the nanotube provides a useful means for individualizations, an in-depth understanding the π-π interaction between conjugated polymers and the nanotube is of great importance in nanoelectronic applications. Noncovalent attractive π-π interactions between the π–electrons of unsaturated organic systems play a key role in many aspects of modern chemistry, materials science, and biochemistry [1,2].When these interactions occur between parallel oriented π–systems, the term "π-π stacking" is typically used. The simplest prototype system with π-π stacking is the benzene dimer, and thus considerable attention has been dedicated to exploring the structural and electronic properties as a preliminary investigation.

As a soluble π-conjugated polymer, poly[(*m*-phenylenevinylene)-*alt*-(*p*-phenylenevinylene)] (P*m*PV) is a prototype polymer for dispersing SWCNTs [13-24]. Several experimental studies of wrapping SWCNTs with P*m*PV derivatives have been reported, which show selective interactions with SWNTs by diameter and chirality [5,23]. However, the nature of this selectivity due to the non-covalent interaction between P*m*PV and SWCNTs is not fully understood [5]. To understand interfacial chemistry and the dispersion mechanism, we have employed force- field-based molecular dynamics (MD) and first-principles density-functional calculations to study the optimum geometry and electronic interaction between a pair of benzene molecules, which is essential in P*m*PV wrapped SWCNTs. Force-field-based MD was used to investigate the wrapping process and the binding properties, and first-principles calculations were employed to determine the electronic structure.

Our results demonstrate that the semi-rigid π-conjugated polymer

backbone is flexible enough to adjust its conformation during successive helical wrapping. The helical-wrapping induced effective dispersion is critical for enabling the development of nanodevices with optimized properties, and developing multifunctional nanocomposites capable of bearing structural loads and functioning as sensors.

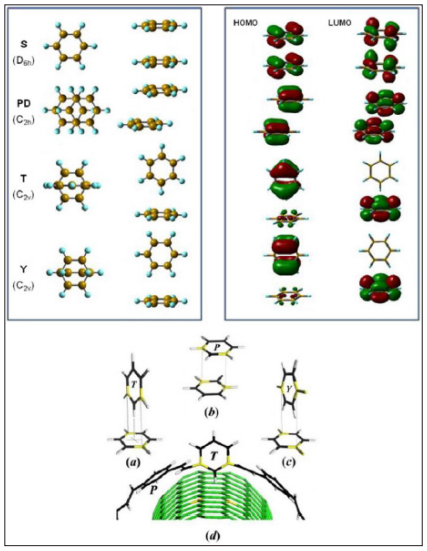


**Figure 1**: (Top panel) Optimized structure of sandwich *S* ($D_{6h}$), parallel displaced PD ($C_{2h}$), *T* ($C_{2v}$) and *Y*-shaped *Y* ($C_{2v}$) structures along with the charge density of each shape for highest occupied molecular orbital (HOMO) and lowest unoccupied molecular orbital (LUMO). (Bottom panel) Optimized structures of T-shaped, Y-shaped, parallel-displaced benzene pair and a phenylene (of P*m*PV) on SWCNT.

## Methods

All our calculations have been performed using the Gaussian 03, Materials Studio 5.5, and TeraChem 1.0packages [25-28]. The structures of isolated benzene monomers and various geometrical conformations of the benzene dimers were optimized using B3LYP methodwith 6-311G and 6-311++G basis sets, second order Møller–Plesset perturbation (MP2)with 6- 31G (d,p) polarized valence basis set or aug-cc-pVDZ polarized valence basis set with augmented diffuse functions [29-32]. The energy minimum for all optimized structures was confirmed from vibrational frequency analysis. All geometry optimizations and single-point calculations utilized the frozen core approximation. The conformations were optimized at the MP2/6- 31G (d,p) level that were subsequently used for the calculations of dimmers interaction energies. The single-point energy calculations, including calculations of the interaction energies for all dimmers, have been performed in the framework MP2/aug-cc-pVDZ approach. Basis set superposition error (BSSE) correction has been taken in to account by the counterpoise method (CP). Moreover, three-body electron correlations, described by triple excitations relative to the reference configuration, are also significant. Hence, coupled-cluster computations with perturbative triples [CCSD (T)] have also been performed and combined with the Hartree-Fock and MP2- R12/A values to estimate complete basis CCSD (T) binding energies for benzene dimer, which should be accurate to a few tenths of a kilocalorie per mole. In addition, calculations were performed within DMol3 approachwith triple numerical polarized (TNP) basis functions and empirical dispersion corrected density-functional approaches [26].

The structure and electronic properties of different conformations were investigated using dispersion-corrected first-principles density-functional calculations [33]. We used the Perdew- Burke-Ernzerhof (PBE) parameterization of the generalized gradient approximation (GGA). The general-gradient-approximation (GGA) results were subsequently rectified through the inclusion of dispersion correction [34,35]. Tkatchenko-Scheffler (TS) dispersion correction accounts for the relative variation in dispersion coefficients of differently bonded atoms by weighting values taken from the high-quality *ab-initio* database with atomic volumes derived from partitioning the self-consistent electronic density. The TS scheme exploits the relationship between polarizability and volume. The inclusion of dispersion-correction is essential to describe the non-covalent interactions between P*m*PV and SWCNTs correctly.

A kinetic energy cutoff of 280 eV in the plane-wave basis and a kinetic energy tolerance less than $3\times10^{-4}$eV in the orbital basis, and appropriate Monchorst-Pack *k* -points (1×1×10) were sufficient to converge the grid integration of the charge density. The initial search for stable structures was carried out through force-field based molecular dynamics [36]. The resultant structures were further optimized through first-principles calculations with forces less than 0.01 eV/Å with plane wave basis. We used force-field based molecular dynamics for geometry optimization. Geometry optimization calculations were employed using conjugated gradient.

## Results

We have investigated the structures of the benzene dimer using different level of the theory, including accurate MP2 method with extended basis set and less expensive dispersion-corrected first-principles density-functional calculations [25-36]. We have used the Perdew-Burke-Ernzerhof (PBE) parameterization of the generalized gradient approximation (GGA) double numerical (DN) basis set [25]. For geometry optimization, the starting geometries of the dimer were built up taking into account the well-known sandwich *S* ($D_{6h}$), parallel displaced *PD* ($C_{2h}$), *T*-shaped ($C_{2v}$), and *Y*-shaped (C2v) structures (see Fig 1 top panel). After initial optimization, the imposed symmetry constraint was released. Coupled with intensive simulated annealing, three low-energy structures *PD*-A ($C_1$), *PD*-B ($C_1$), and *Y*-displaced *YD* ($C_1$) were obtained (Figure. 2).

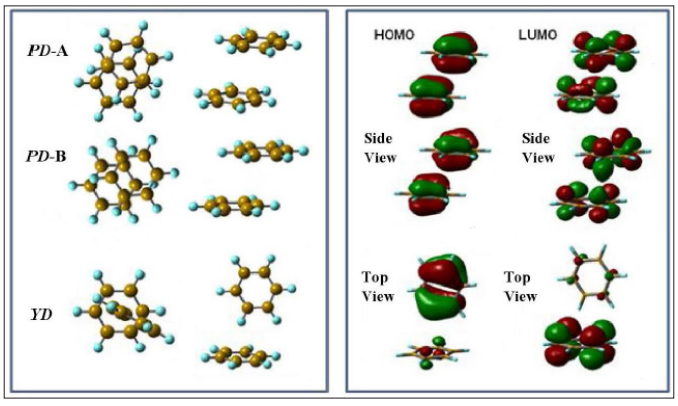


**Figure 2**: Optimized structures and charge density plots of lowest energy conformations (parallel displaced (*ortho* direction) *PD*-A, parallel displased (*meta* direction) *PD*-B and Y -shaped).

We show in Figure 1 the optimized structures of a benzene pair. In the simple model of aromatic π-π interactions, two interacting benzene rings can be aligned in parallel displaced *P* (Figure 1b)

or perpendicular geometry (edge-to-surface interaction). As seen from Figure 1, in the conformation *S* and *PD*, the planes of the two benzene rings are virtually parallel to each other while one of the rings in structure *PD* is displaced in the *ortho* direction. The parallel arrangement of the electronic charges favors the π-π stacking interaction between the benzene monomers. The same is true for *PD*-A and *PD*-B as well (see Figure. 2), which can be obtained from *S* by in-plane shifting of one of the monomers in two different directions, followed by a small rotation of the displaced benzene ring.

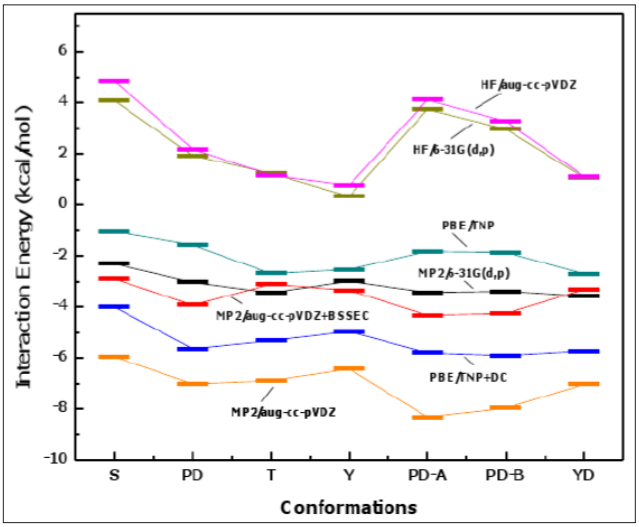


**Figure 3**: Interaction energies of sandwitch (*S*), parallel displaced (*PD*), *T*-shaped (T), *Y*-shaped (*Y*), Parallel Displaced (*ortho* direction) (*PD*-A), parallel displaced (*meta* direction) *PD*-B and *Y*-displaced (*YD*) structures with MP2/aug-cc-pVDZ, PBE/TNP+DC, MP2/aug-ccpVDZ+ BSSEC, MP2/6-31G(d,p), PBE/TNP, HF/6-31G(d,p) and HF/aug-cc-PVDZ methods.

The difference between these two conformations is that one of the benzene monomers in *PD*-A and *PD*-B is displaced along *ortho* and *meta* directions, respectively. The edge-to-surface interaction can be further classified into the *T*-shaped (Figure. 1a) or *Y*-shaped conformations (Figure 1c). In *T*-shaped structure, a hydrogen atom on a benzene ring is pointing towards the center of another ring. In the *Y*-shaped conformation, two of the hydrogen atoms on a benzene ring are pointing to the two carbon atoms of another ring.

Recent studies in π-π interactions of aromatic liquids reveal that benzene-benzene interaction geometry depends on separation distance [37-39]. At small molecular separations (< 5 Å) there is a preference for parallel π-π contacts (*P*-shaped) in which the molecules are offset to mimic the interlayer structure of graphite. At larger separations (> 5 Å) the adjacent aromatic rings are predominantly perpendicular (*Y*-shaped), with two H atoms per molecule directed toward the acceptors π- orbitals. It is worth noting that so-called anti-hydrogen-bond configuration (*T* shaped), which was proposed theoretically as the global minimum for the benzene dimer, occurs only as a saddle point in the experimental study [37-39]. Quantum chemistry calculation results suggest that the off-centered parallel displaced and *T*-shaped structures are nearly degenerated [40-44]. Molecular dynamic studies confirm that off-centered parallel-displaced or *T* shaped structures are favorable depending on the magnitude of the partial charges used in the electrostatic model [45]. Small charges stabilize parallel displaced geometries while the large partial charges favor *T*-shaped structures [45].

Illustrated in Figure 3 are extracted energies from various levels of theory. Initially, we have performed geometry optimizations for the ground states of the conformers using Hartree-Fock method (HF) with the basis set 6-311++G. The finding confirms that HF underestimates the π-π stacking interaction. The analysis of the results obtained at MP2/aug-cc-pVDZ+BSSEC level show that the most stable conformations are non-symmetrical parallel displaced structure PD-A, and PD-B [37]. The interaction energies for these dimers are -4.3 and -4.2 kcal/mol, respectively. Slightly higher in energy is the parallel displaced structure PD, with interaction energy of -3.9 kcal/mol. The T-shaped and Y-shaped structures are almost isoenergetic (-3.1 and -3.4 kcal/mol) with the *YD* structure (-3.3 kcal/mol) and significantly higher in energy than *PD* conformations. The perfectly stacked structure *S* is much less stable, with an interaction energy of -2.9 kcal/ mol. The analysis of the obtained result shows that the relative energies of these 7 configurations are similar, indicating a very flat potential energy surface. The lowest energy structures are *PD*-A and *PD*-B. The S configuration is the least favorable of the seven geometries examined. It is remarkable to see from Figure. 3 that computationally much less expensive PBE/TNP method with dispersion correction show results qualitatively similar to that obtained using time consuming MP2/aug-cc-pVDZ+BSSEC approach.

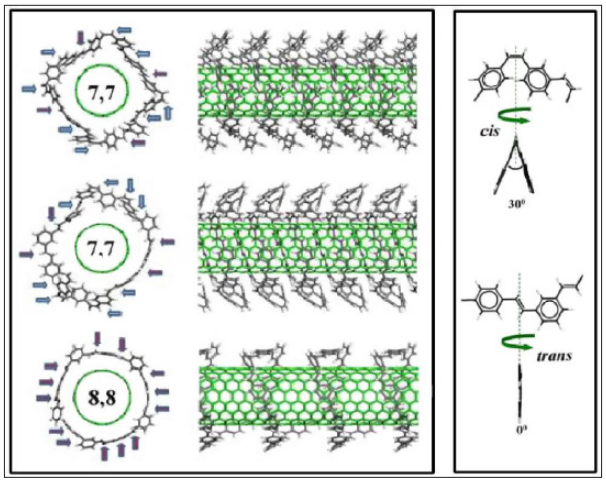


**Figure 4**: Left panel: Optimized structures of wrapped *cis*-P*m*PV (*trans*: *cis* ratio 1:2; left panel top figure), *cis*-P*m*PV (*trans*: *cis* ratio 2:4), and *trans*-P*m*PV around SWCNT (left panel bottom figure). Right panel: *cis* and *trans* monomers of P*m*PV.

Closer scrutiny of the locally stable configurations displays in Figure. 1d reveal that the phenylene fragments are arranged either perpendicularly or parallel to the SWCNT surface. Parallel or perpendicular assembly facilitates the π-π interactions

As seen from Figure. 1d, the *meta*-linked benzene ring tends to adopt *T*-shaped or its slanted variant. The *para*-linked benzene ring can adopt either *P*- or *Y*-shaped configurations, depending on the chirality of the nanotube, as well as the wrapping pattern. Specifically, the stereoisomers, *cis* and *trans*, play an important role in the wrapping pattern and also contribute to the availability of *T*-shaped, *P*-shaped or *Y*-shaped configurations in the hybrid.

Experimental results indicate that the benzene rings in cis-P*m*PV prefer perpendicular orientations to the SWCNTs, as predicted from the extended π-conjugation along the polymer chain [46].

It is assumed that the *meta*-linked phenylene ring adopts the perpendicular orientation (to SWCNT surface), as the bent angle at the *meta*-phenylene provides necessary curvature to wrap SWCNT. Benzene rings that are connected at their '*para*' positions (i.e. *para*-phenylene), however, can adopt either perpendicular or parallel orientation to SWCNT surface. The ratio of *para*-phenylene in perpendicular and parallel orientation is dependent on the local polymer- SWCNT interaction. The *cis*- and *trans*-vinylene bond geometry may also affect the ratio of perpendicular and parallel orientation of *para*-phenylene. Repeating unit of *trans*- and *cis* vinylene stereoisomers of a P*m*PV are shown in Figure. 4 right panel. In the *trans* isomer, two benzene rings are in the same plane. Two benzene rings in the *cis* isomer, however, are rotated away from each other by 30° angle, due to the steric hindrance. In other words, the two phenylene rings in the *cis* isomer are forced to rotate away significantly from the *co*-planarity. The dihedral angle between the two phenylene planes remains unchanged after wrapping around the SWCNTs (Figure. 4 left panel). In one aspect, polymer chain rigidity, as a consequence of the extended π-conjugation, prevents the parallel positioning of the benzene rings.

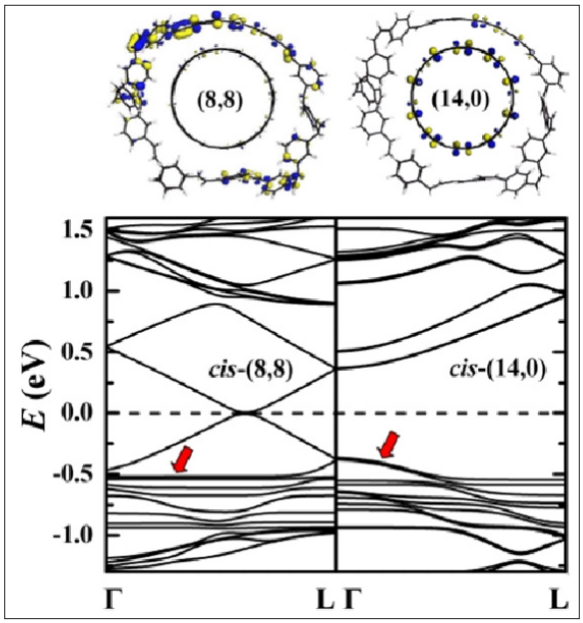


**Figure 5**: Top panel: charge density plots of *cis*-P*m*PV around the metallic (8,8) and semiconducting (14,0) SWCNTs. Bottom panel: Calculated electronic band structure for *cis*- P*m*PV, with metallic (8,8) and semiconducting (14,0) SWCNTs.

We have investigated two types of polymer chains according to their concentration of cis and trans isomers linkages by considering two monomer units shown in Figure 4. The polymerchain, referred to as *cis*-P*m*PV, has a 1:2 ratios between *trans* and *cis* monomer units. The polymer chain, referred to as *trans*-P*m*PV, has a trans configuration throughout the polymer chain. Furthermore, we have examined configurations with different *trans* and *cis* units for *cis*-P*m*PV, specifically 1:2 and 2:4 ratios, to assess the stability of the nanohybrids. The selfassembledpolymer chains, which are wrapped helically around the nanotube, result in a very short pitch for *cis*-P*m*PV (Figure 4).

In other words, *cis*-P*m*PV is wrapping SWCNT more tightly than *trans*-P*m*PV. The shorter the pitch of the polymer wrapped around SWCNTs, the more efficient is the dispersion. Our calculation results indicate that *trans*-P*m*PV (Figure. 4 bottom) has a 2.5 nm pitch, in good agreement with experimental observations [46]. On the other hand, we have found that *cis* P*m*PV has a 1.5 nm pitch length. The difference in pitch length is in agreement with experimental findings that the *trans*:*cis* isomer ratio 1:2 yields stronger interactions between the polymer and the tube. The wrapping pattern is rigid in *cis*-P*m*PV due to the fixed angle between the two benzene rings in the monomer unit.

In general, the wrapped structure assumes an n-fold polygonal shape where the number of polymer units wrapped around the nanotube is related to the tube diameter and the side-chain length. The *trans*-P*m*PV isomer prefers the SWCNTs with large diameters because larger tubes have bigger contact area. Hence, the *trans*-P*m*PV isomer with higher chain rigidity shows better selectivity in comparison to the more flexible *cis*-P*m*PV wrapping. Therefore, the orientation order plays a nonessential role in the selectivity of the SWCNTs. The P*m*PV conformation as shown in Figure 4 has 13 and 14 Meta and para linkages, respectively. It was observed that para linkages prefer to be parallel to the surface of the tube while the Meta linkages are slanted to the surface of the nanotube. Side chains play a significant role in the wrapping of P*m*PV along the SWCNT, for connectivity in between the side chains affects the bonding to the polymer chain. Side chains with donor-acceptor interactions lead to the successful selectivity of SWCNTs. There is a great chance for *para*-linked benzene rings to adopt *Y*-shaped over *P*-shaped configurations after wrapping around SWCNTs, following the behavior of pairs of aromatic rings. The side chains are attached to the *para*-linked benzene rings in their meta and *ortho* positions. The interactions of side chains limited the rotations of the *para*-linked benzene rings in the *trans*-P*m*PV polymer and thus lower the available *Y*-shaped configurations.

In Figure 5, we present the calculated electronic band structure for *cis*-P*m*PV, interacting with metallic (8,8) and semiconducting (14,0) SWCNTs, respectively. The charge density plots indicate that the charges are localized in the polymer chain of the cis-P*m*PV/ (8,8)-SWCNT hybrid. This observation is supported by the degree of dispersion in the HOMO-derived band (highlighted red arrows in Figure. 5). For the *cis*-P*m*PV/ (14,0)-SWCNT hybrid, charge densities are predominantly concentrated on the tube. These findings indicate that the *cis*-P*m*PV polymer primarily shows a preference for metallic tubes. The hypothesis is also supported by the calculated binding energies shown in Table 1.

Another important aspect of this study is to clarify the relative stability of T-shape, slanted Tshape, or parallel dispersed benzene dimer configurations. For this reason, we have studied three different conformations of *trans*-P*m*PV polymer wrapped SWCNTs. These conformations include *all*-vertical-*T* (the polymer conformation with all of the benzene rings are vertical to the SWCNT surface), *half*-vertical-*H* (the polymer conformation with half of the benzene rings are vertical to the SWCNT surface), and the parallel-*P* (the polymer conformation with all the benzene rings are parallel to the SWCNT) conformations.

**Table 1: Calculated binding energy differences in eV with respect to the lowest energy conformation by using LDA ($E_{LDA}$) and GGA ($E_{GGA}$) parametrization, energy gap between HOMO and LUMO ($E_g$), Length of the SWCNT (L) and diameter of the SWCNT (d).**

| Structure | $E^{LDA}$ (eV) | $E^{GGA}$ (eV) | Eg | L (Å) | d (Å) |
|---|---|---|---|---|---|
| H-trans (8,8) | - | 0.63 | 0 | 12.3 | 3.4 - 3.9 |
| P-trans (8,8) | 1.07 | - | 0 | 12.3 | 3.3 - 3.7 |
| H-trans (8,8) | 3.32 | 5.85 | 0 | 12.3 | 3.8 - 5.4 |
| H-trans (14,0) | - | 0.18 | 0.75 | 12.8 | 3.3 - 3.7 |
| P-trans (14,0) | 0.37 | - | 0.75 | 12.8 | 3.2 - 3.5 |
| H-trans (14,0) | 3.35 | 4.96 | 0.76 | 12.8 | 3.6 - 5.1 |
| cis(8,8) | - | - | 0 | 6.6 | 3.0 - 6.3 |
| cis(14,0) | 1.22 | 4.64 | 0.75 | 6.9 | 2.9 - 6.0 |

Dash (-) represents the lowest energy conformation in each calculation.

Summarized in Table 1 are the calculated diameters, along with the band gap values for various conformations of the π-conjugated *trans*-P*m*PV polymer chains interacting with the SWCNTs. The total energy order for each structure conforms to force-field-based MD calculation results. We compared the pitch of the helically wrapped polymer chains and the van der Waal distances between the polymer and the nanotube. We also show in Table 1 the binding energies of the different conformation with respect to the corresponding lowest energy conformation for each tube. As seen from Table 1, the relative stability of half (*H*) and *all*-vertical (*T*) conformations depends on the calculation methods.

Specifically, with the use of GGA exchange-correlation, the parallel conformations are preferred. By contrast, with the use of LDA as the exchange-correlation then the *half*-vertical conformations are preferred. The polymer conformation with all the benzene rings perpendicular to the SWCNT (*T-trans)* is not a low energy conformation. Calculations reveal the all vertical is not preferred, although it is more tightly wrapped around. The smaller helical pitch of *cis*-P*m*PV is nearly half that of the *trans*-P*m*PV conformation. The tight wrapping pattern is in agreement with the experimentally observed high dispersion of the tubes onto the polymer. Band structure of *trans*-P*m*PV polymer wrapped metallic-SWCNTs contains both dispersed bands and flat bands (Figure. 5). Flat bands originate from the P*m*PV and dispersed bands originate from SWCNTs. Valence bands are affected due to the hybridization of SWCNTs bands with the *trans*- P*m*PV polymer flat bands, which allow for the observation of the highest occupied molecular orbital (HOMO)-derived bands. These findings imply that the P*m*PV polymer acts primarily as an electron donor to SWCNTs. We have plotted the charge density together with band structures and found that hybridization is strong when the parallel conformation conjugated with the metallic tubes, followed by the vertical, half vertical conformations, respectively.

We illustrate in Figure. 6 the characteristic features of the electronic structures of the semiconducting-SWCNT wrapped with a *trans*-P*m*PV polymer. The distribution of the HOMO-derived band, in the occupied states, continuously increases starting from half-vertical, parallel, and then to *all*-vertical conformations after interacting with the semiconducting SWCNT (Figure. 6) For the case of semiconducting SWCNTs, calculated charge densities for the homo-derived bands indicate that the hybridization is higher in the *half*-parallel and parallel conformations of P*m*PV compared to that of the all vertical conformations.

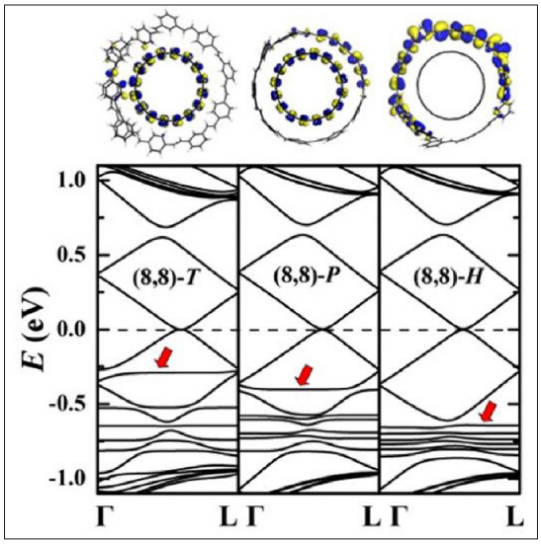


**Figure 6**: Top panel: charge density plots of *trans*-P*m*PV with all vertical benzene rings (*T*), parallel benzene rings (*P*) and half vertical benzene rigs (*H*) around the metallic (8,8) SWCNT. Bottom panel: Calculated electronic band structure for trans-P*m*PV, with metallic (8,8) SWCNT.

In summary, we performed a systematic modeling study that provides crucial insights into the selective interactions between SWCNTs and π-conjugated polymers. Since the diameter and chirality of the nanotubes dictate their mechanical properties as well as electrical conductivity, an in-depth understanding of the interactions between conjugated polymers and carbon nanotubes is of great importance. The study reveals that the *cis*- and *trans*-*v*inylene bond geometry plays an important role to influence the orientation of the polymer's phenyl rings toward SWCNT. When P*m*PV is wrapping around an SWCNT, the optimum polymer-SWCNT interaction appears to be dependent on the molecular ability to adjust the orientation of phenyl ring, which is essential for achieving optimum interaction via adopting *Y*- or *PD*-interactions (listed in Figure. 1). The approach thus shed light on the details of intermolecular interaction between P*m*PV and SWCNT, which can be employed to the novel π-conjugated polymers. Investigation of relevant structural and electronic properties is important for the development of nanotube based Nano electronics and nanostructured composites.

## Acknowledgment

This work was supported by the National Science Foundation (Grant Nos. DMR-0934142, HRD- 1137751, and DMR-1539918) and the work used the Extreme Science and Engineering Discovery Environment (XSEDE) Stampede2 at the TACC and Super MIC at LSU through allocation DMR120078.

## References

1. Odom TW, Huang JL, Kim P, Lieber CM (1998) Atomic Structure and Electronic Properties of Single-Walled Carbon Nanotubes, Nature 391: 62-64.
2. Dresselhaus MS, Dresselhaus G, Avouris P (2001) Carbon Nanotubes: Synthesis, Structure, Properties, and Applications, Springer Berlin. ISBN 978-3-540-39947-6.
3. Ajayan PM (1999) Nanotubes from Carbon, Chem. Rev 99: 1787-1800.
4. Papadimitrakopoulos F, Ju SY (2007) Materials Science: Purity Rolled Up in a Tube, Nature 450: 486-487.
5. Kim SN, Luo Z, Papadimitrakopoulos F (2005) Diameter and Metallicity Dependent RedoxInfluences on the Separation of Single-Wall Carbon Nanotubes, Nano Lett 5: 2500-2504.
6. Zheng M, Semke ED (2007) Enrichment of Single Chirality Carbon Nanotubes, J. Am. Chem. Soc129: 6084-6085.
7. Zheng M, Jagota A, Semke ED, Diner BA, Mclean RS, et al. (2003) DNA-Assisted Dispersion and Separation of Carbon Nanotubes, Nature Mater 2: 338-342.
8. Ju SY, Doll J, Sharma I, Papadimitrakopoulos F (2008) Selection of Carbon Nanotubes with Specific Chiralities Using Helical Assemblies of Flavin Mononucleotide, Nat. Nanotechnol 3: 356-362.
9. Kim SN, Kuang Z, Grote JG, Farmer BL, Naik RR (2008) Enrichment of (6,5) Single Wall Carbon Nanotubes Using Genomic DNA, Nano Lett8: 4415-4420.
10. Tu X, Manohar S, Jagota A, Zheng M(2009) DNA Sequence Motifs for Structure- Specific Recognition and Separation of Carbon Nanotubes, Nature 460: 250-253.
11. Nish A, Hwang JY, Doig J, Nicholas RJ(2007) Highly Selective Dispersion of Single-Walled Carbon Nanotubes Using Aromatic Polymers, Nat. Nanotechnol 2: 640 646.
12. Yi W, Malkovskiy A, Chu Q, Sokolov AP, Colon ML, et al. (2008) Wrapping of Single-Walled Carbon Nanotubes by a π-Conjugated Polymer: The Role of Polymer Conformation-Controlled Size Selectivity, J. Phys. Chem. B 112: 12263-12269.
13. Chen Y, Malkovskiy A, Wang XQ, Colon ML, Sokolov AP, et al. (2012)Selection of Single-Walled Carbon Nanotube with Narrow DiameterDistribution by Using a PPE–PPV Copolymer, ACS Macro Lett 1: 246-251.
14. Keogh SM, Hedderman TG, Lynch P, Farrell GF, Byrne HJ (2006) Bundling and Diameter Selectivity in HiPco SWNTs Poly(p-phenylene vinylene-co-2,5-dioctyloxy mphenylenevinylene) Composites, J. Phys. Chem. B 110: 19369-19374.
15. Keogh SM, Hedderman TG, Farrell G, Byrne HJ (2004) Spectroscopic Analysis of Single-Walled Carbon Nanotubes and Semiconjugated Polymer Composites, J. Phys. Chem.B 108: 6233-6241.
16. Pang Y, Li J, Hu B, Karasz FE (1999) A Highly Luminescent Poly(mphenylenevinylene)-alt- (p-phenylenevinylene) with Defined Conjugation Length andImproved Solubility, Macromolecules 32: 3496-3950.
17. Saebo S, Almolof J, Boggs JB, Stark JG (1989) Two Approaches to The ComputationalDetermination of Molecular Structure: The Torsional Angle in Tolane and The Effect ofFluorination On the Structure of Oxirane, J. Mol. Struct 200: 361-373.
18. Chen J, Liu H, Weimer WA, Halls MD, Valdeck DH, et al. (2002)Noncovalent Engineering of Carbon Nanotube Surfaces by Rigid, Functional ConjugatedPolymers, J. Am. Chem. Soc124: 9034-9035.
19. Bargen CDV, MacDermaid CM, Lee OS, Deria P, Therien MJ, et al (2013) Origins of the Helical Wrapping of Phenyleneethynylene Polymers about Single WalledCarbon Nanotubes, J. Phys. Chem. B 117: 12953-12965.
20. Furmanchuk A, Leszczynski J, Tretiak S, Kilina SV (2012) Morphology and OpticalResponse of Carbon Nanotubes Functionalized by Conjugated Polymers, J. Phys. Chem. C116: 6831-6840.
21. Chen Y, Xu Y, Perry K, Sokolov AP, More K, et al. (2012) Achieving Diameter Selective Separation of Single-Walled Carbon Nanotubes by Using Polymer Conformation-Confined Helical Cavity, ACS Macro Lett 1: 701-705.
22. Bilalis AP, Katsigiannopoulos D, Avgeropoulos A, Sakellariou G (2014) Non-CovalentFunctionalization of Carbon Nanotubes with Polymers, RSC Adv 4: 2911-2934.
23. Ponnamma BD, Sadasivuni KK, Grohens Y, Guo Q, Thomas S(2014) CarbonNanotube Based Elastomer Composites – an Approach Towards Multifunctional Materials, J.Mater. Chem. C 2: 8446-8485.
24. SoleymanRC, Adeli M (2015) Impact of Dendritic Polymers OnNanomaterials, Polym.Chem 6: 10-24.
25. MJ Frisch, GW Trucks, HB Schlegel, GE Scuseria, MA Robb, et al. (2004) Gaussian 03, Revision C.02, Gaussian, Inc.,Wallingford CT, http://gaussian.com/g03citation/.
26. DMol3 (2010) Accelrys Software Inc., San Diego, CA,http://accelrys.com/about/newspr/1010-ms-55.html.
27. Kleis J, Hyldgaard P, Schröder E (2005) Van der Waals Interaction of Parallel Polymersand Nanotubes, Comput. MaterSci 33: 192-199.
28. Kleis J, Schröder E (2005) van der Waals Interaction of Simple, Parallel Polymers, J. ChemPhys122: 164902-1-7.
29. Becke AD (1993) Density-Functional Thermochemistry. III. The Role of Exact Exchange, J Chem. Phys 98: 5648-5652.
30. Lee A, Yang W, Parr RG (1988) Development of the Colle-Salvetti Correlation-Energy Formula into a Functional of the Electron Density, Phys. Rev. B 37: 785-789.https://doi.org/10.1103/PhysRevB.37.785.
31. Møller A, PlessetMS (1934) Note on an Approximation Treatment for Many-Electron Systems, Phys. Rev 46: 618-622. https://doi.org/10.1103/PhysRev.46.618.
32. Hohenberg P, Kohn W (1964) Inhomogeneous Electron Gas, Phys. Rev 136: 864-871. https://doi.org/10.1103/PhysRev.136.B864.
33. Payne MC, Teter MP, Allan DC, Arias TA, Joannopoulos TD (1992) IterativeMinimization Techniques for Ab Initio Total-Energy Calculations: Molecular Dynamics andConjugate Gradients, Rev. Mod. Phys 64: 1045-1097.
34. Perdew J, Burke K, Ernzerhof M (1996) Generalized Gradient Approximation Made Simple, Phys. Rev. Lett 77: 3865-3868.
35. Tkatchenko A, Scheffler M (2009) Accurate Molecular Van Der Waals Interactions from Ground-State Electron Density and Free-Atom Reference Data, Phys. Rev. Lett 102: 073005-1-4.
36. Tersof J (1988) New Empirical Approach for The Structure and Energy of Covalent Systems,Phys. Rev. B 37: 6991-7000.
37. Headen TF, Howard CA, Skipper NT, Wilkinson MA, Bowron

DT, et al (2010) Structure of π–π Interactions in Aromatic Liquids, J. Am. Chem. Soc 132: 5735-5742.
38. Grimme S (2008) Do Special Noncovalent π–π Stacking Interactions Really Exist?,Angew.Chem. Int. Ed 47: 3430-3434. https://doi.org/10.1002/anie.200705157.
39. Sinnokrot MO, Sherill CD (2006) High-Accuracy Quantum Mechanical Studies of π–π Interactions in Benzene Dimers, J. Phys. Chem. A 110: 10656-10668.
40. Hobza P, Selzle HL, Schlag EW (1994) Potential Energy Surface of the Benzene Dimer: Ab Initio Theoretical Study, J. Am. Chem. Soc116: 3500-3506.
41. Tsuzuki S, Uchimaru T, Mikami M, Tanabe K (1996) Basis Set Effects On the CalculatedBonding Energies of Neutral Benzene Dimers: Importance of Diffuse Polarization Functions,Chem. Phys. Lett 252: 206-210.
42. Jafe RL, Smith GD (1996) A Quantum Chemistry Study of Benzene Dimer, J. Chem. Phys 105: 2780-2788. https://doi.org/10.1063/1.472140.
43. Chipot C, Jafe R, Maigret B, Pearlman DA, Kollman PA (1996) Benzene Dimer: A Good Model for π–π Interactions in Proteins? A Comparison between the Benzene and the Toluene Dimers in the Gas Phase and in an Aqueous Solution, J. Am. Chem. Soc 118: 11217-11224. 10.1021/ja961379l.
44. Hobza P, Selzle HL, Schlag EW (1996) Potential Energy Surface for the Benzene Dimer. Results of ab Initio CCSD(T) Calculations Show Two Nearly Isoenergetic Structures: TShapedand Parallel-Displaced, J. Phys. Chem100: 18790-18794. 10.1021/jp961239y.
45. Bernstein ER: Sun SJ (1996) Aromatic van der Waals Clusters: Structure and Nonrigidity, J. Phys. Chem 100: 13348-13366. 10.1021/jp960739o.
46. Yi W, Malkovskiy A, Xu Y, Wang X, Sokolov AP (2010) Polymer Conformation-Assisted Wrapping of Single-Walled CarbonNanotube: The Impact of cis-Vinylene Linkage, Polymer 51: 475-481.https://doi.org/10.1016/j.polymer.2009.11.052.